Nonradiative Quenching of Fluorescence in a Semiconducting Carbon Nanotube: A Time-Domain *Ab Initio* Study

Bradley F. Habenicht and Oleg V. Prezhdo*

Department of Chemistry, University of Washington, Seattle, Washington 98195-1700, USA

(Received 13 September 2007; published 14 May 2008)

As shown experimentally, strong nonradiative decay channels exist in carbon nanotubes (CNT) and are responsible for low fluorescence yields. The decay of the electronic excitation to its ground state is simulated in the (6,4) semiconducting CNT with surface hopping in the Kohn-Sham representation, providing a unique time-domain atomistic description of fluorescence quenching. The decay in the ideal CNT is estimated to occur on a 150 ps time scale and is only weakly dependent on temperature. Vibrationally induced decoherence strongly influences the electronic relaxation. Defects decrease the excited state lifetime to tens of picoseconds, rationalizing the multiple decay time scales seen in experiments.

DOI: 10.1103/PhysRevLett.100.197402 PACS numbers: 78.67.Ch, 31.10.+z, 71.38.-k, 73.22.-f

Ever since the first report in 2002 [1], photoluminescence (PL) from isolated carbon nanotubes (CNT) has received much study. In the last five years, CNTs have fluoresced in micelles [1], silicon pillars [2], polymer matrices [3], and gelatin [4]. The temperature and *p*H dependence of the PL has been investigated [1,4–10]. In spite of the significant efforts from across the world, there exists major uncertainty in these reports. Quantum yields have varied between 10^{-4} [3,11], 10^{-3} [12], up to 7% [13]. Observed PL times show multiexponential decays with components ranging from tens of picoseconds to nanoseconds [3,4,12,14,15]. Experimentally estimated radiative lifetimes are in the tens to hundreds of nanoseconds [5,6,11,12], while theory has produced lifetimes which vary from hundreds of picoseconds to ten nanoseconds [16,17]. The community agrees that nonradiative decay channels must be active in CNTs, as evidenced by the low PL quantum yields and multiexponential decays, and several nonradiative decay models have been proposed [5,15]. The large spread in the PL times and yields leaves much to be explained, and further theoretical and experimental investigations are clearly necessary.

The present letter reports the first time-domain *ab initio* study of the nonradiative fluorescence quenching in CNTs, directly mimicking the time-resolved experiments [3–6,8–12,14]. Made possible by the recent theoretical development [18,19], the study combines the time-domain density functional theory [20] (TDDFT) with the fewest switches surface hopping (FSSH) [21,22]. The current approach extends one step further by incorporating quantum decoherence effects, which are known to influence relaxation rates in condensed phase systems [23–25]. The nonradiative decay is investigated for the ideal (6,4) CNT at ambient and low temperatures. In addition, two common defects [26] are considered in order to probe their role in the PL quenching. The simulations show that the ideal tube decays nonradiatively within 150–170 ps, and that the decay is significantly increased by the defects. The relaxation is weakly temperature dependent as it is induced primarily by modes whose frequencies are significantly higher than k_BT. The study indicates that defects may be responsible for the low PL yields and multiple decay components observed in isolated CNTs.

The study focuses on the chiral (6,4) CNT, which is one of the smallest tubes accessible experimentally [1,3]. The Stone-Wales (SW) defect is a rotation of a C-C bond within the ideal hexagonal lattice, Fig. 1. The 7557 defect represents the insertion of an extra C-C dimer into the lattice. Both C_2 defects disrupt π-conjugation and create two five-membered rings and two seven-membered rings. The geometries of the defect sites are different though, with the dimer insertion creating a stronger distortion. The nonradiative decay in the ideal (6,4) CNT was studied at both 300 and 50 K.

TDDFT-FSSH [18,27] with decoherence was implemented within the Vienna *ab initio* simulation package (VASP) [28]. The electronic density was propagated similarly to the closely related TDDFT studies of CNTs [29,30]. The electron-nuclear energy exchange implemented with FSSH was different and ensured the detailed balance [22], allowing us to study the nonradiative relaxation. As customary with pure DFT functionals [31], the excitation energy was adjusted to the experimental value [3]. The same adjustment was applied to the (6,4) CNT with defects. The electron-hole interactions were included in our approach through the evolution of the electron density and the choice of the DFT functional (GGA). The approaches using the Bethe-Salpeter equation [32] are computationally demanding and cannot yet be used with time-domain electron-phonon dynamics. Our finite temperature simulation predicts that the lowest energy excitation, which is dark and forbidden in the tubes of ideal geometry [32,33], becomes weakly allowed, in agreement with the experiments [8,10,14], due to thermal atomic

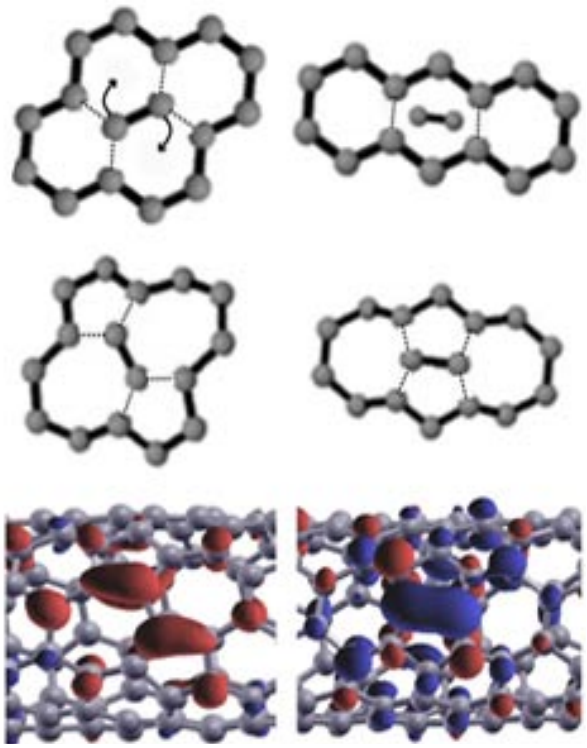

FIG. 1 (color online). Defects imposed on the (6,4) CNT studied in this work. The 7557 defect (right column) is produced by insertion of a C-C dimer across a hexagonal carbon cell. The SW defect (left column) appears due to rotation of one of the C-C bonds. The bottom panels show the transition densities corresponding to the lowest energy excitations generated in the CNT by the defects with the red and blue colors representing positive and negative density changes.

motions that perturb the perfect symmetry of the tube. Our approach showed excellent agreement with the experimental fluorescence linewidths [34] determined by the same electron-phonon interaction that forms the basis for the nonradiative decay studied in present.

By treating nuclei classically, the original FSSH scheme [21,22] excludes coherence loss that occurs in the electronic subsystem by coupling to quantum vibrations. Decoherence can be neglected if it is slower than the electronic transition, for instance, in the subpicosecond relaxation of the higher energy excitations to the lowest excited state [27]. The decay to the ground state is slow, and decoherence must be explicitly included in the quantum-classical simulation. We implemented decoherence within TDDFT-FSSH using a simple semiclassical approach [23,35], which was tested extensively with a variety of condensed phase physical, chemical and biological systems [34,36–38]. The expansion coefficients of the Kohn-Sham wave functions were allowed to evolve coherently up to the decoherence time, at which point they are reset to 0 or 1 with the probabilities given by the squares of coefficients. The decoherence times, estimated as the pure-dephasing times T_2^* in the optical-response or Redfield theory [39], gave good agreement with the experimental PL linewidths [34].

Figure 2 shows the fluctuation of the first excitation energy induced by the nuclear motion. The fluctuation in the ideal (6,4) tube is around 0.1 eV at room temperature and decreases by half-order of magnitude when the temperature is lowered to 50 K. Defects increase the energy fluctuation by a factor of 2, with the C_2 insertion producing a bigger change than the C_2 rotation. This is because defects generate stronger electron-phonon coupling by localizing vibrational modes [26] and electronic states, Fig. 1. The average excitation energy of the ideal tube decreases slightly with increasing temperature due to thermal expansion of the CNT, in agreement with experiments [7,8]. Defects lower the excitation energy.

The electron-phonon coupling is created in the ideal (6,4) CNT by the high-frequency G modes, Fig. 3, both at high and at low temperatures. The SW defect shows disorder modes over a broad range of frequencies [40]. Multiple disorder modes couple to the electronic transition, Fig. 3. In contrast, the excitation localized on the 7557 defect couples primarily to a single low-frequency mode. The insertion of a C-C dimer notably distorts the CNT geometry [26], creating a local mode in the range of low-frequency radial breathing modes.

The nonradiative decay of the lowest excited electronic state gives rise to the ground state population, Fig. 4.

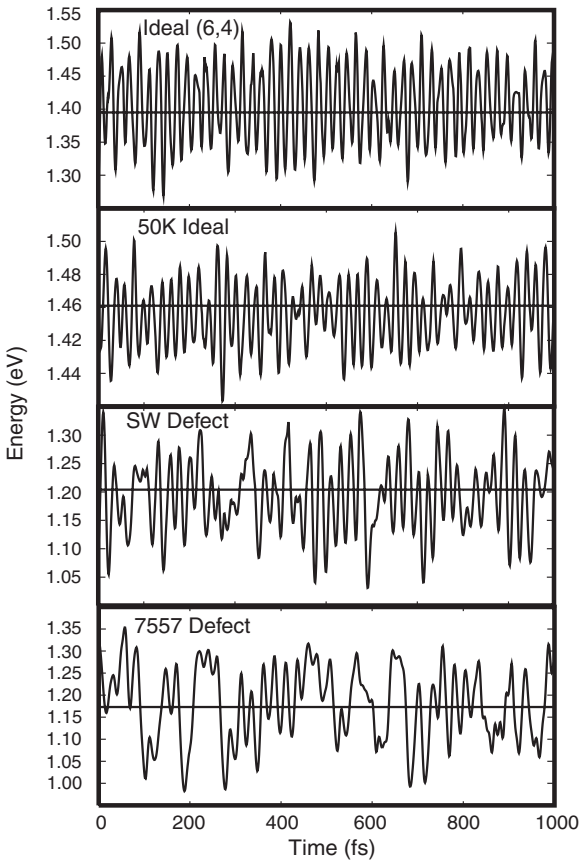

FIG. 2. Phonon-induced fluctuation of the lowest excitation energy of the CNTs used in this study. Note the different energy scales in each panel.

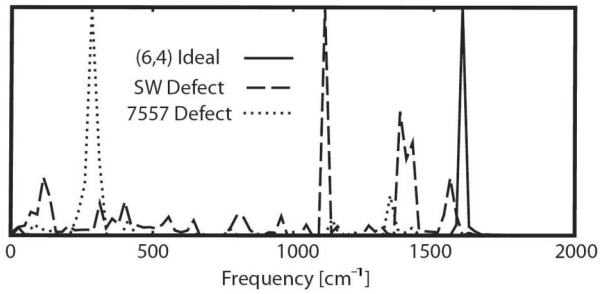

FIG. 3. Fourier transforms of the excitation energies shown in Fig. 2.

Assuming that the full nonradiative decay is exponential, as observed in the experiments [3–6,11,12,14,15], we fitted the 3 ps component available from the simulation to $P(t) = 1 - \exp(t/\tau) \approx t/\tau$ and obtained the nonradiative relaxation times τ reported in Table I. The relaxation time shows strong dependence on the pure-dephasing or decoherence time, because the dephasing occurs faster than the relaxation. The nonradiative lifetime estimated for the ideal (6,4) tube at room temperature is around 150 ps, falling within the experimental range [3–6,11,12,14,15]. The defects substantially accelerate the relaxation, reducing the lifetime to tens of picoseconds and providing a rationalization for the multiple decay components observed in the experiments. For example, Refs. [3,4] report two sets of decay times around 10–20 ps and 180–300 ps, see Fig. 2(g) of [3] and Fig. 2(c) of [4], respectively. Our calculations indicate that the longer times correspond to pristine tubes, while the shorter times are due to defects. The bond insertion, 7557 defect, has a more profound effect on the relaxation process than does the bond rotation SW defect.

The influence of defects on the electron-phonon relaxation can be traced to the following three factors. First, defects lower the excitation energy, Fig. 2. Second, they create localized and strongly coupled electronic states and vibrational modes, Figs. 1 and 3. Third, defects accelerate dephasing, Table I. The first two factors act to speed up the relaxation by creating a better electron-phonon energy match and a larger coupling. The third factor slows the relaxation in general, as exemplified by the quantum Zeno effect [23,41,42], although counter-examples are known [24,42]. Overall, the defects accelerate the relaxation, which is consistent with the recently observed quenching of mobile excitons at localized sites [43].

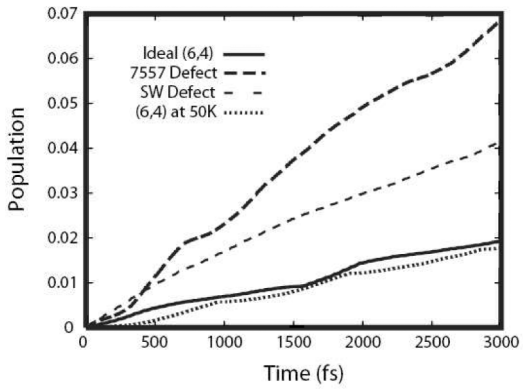

FIG. 4. Population of the ground electronic state in the CNTs studied as a function of time. $T = 300$ K, except for the dotted line.

The nonradiative decay shows little temperature dependence, Fig. 4 and Table I. This is not surprising, since the relaxation is induced by the modes whose frequencies are significantly higher than $k_B T$ at the relevant temperatures [5]. Our semiclassical approach reproduced the weak temperature dependence [5,6,8,9], emphasizing the role of decoherence in the quantum-classical simulation [23,35]. The decay rate is determined by the product of the electron-phonon coupling matrix element squared and the correlation function for the phonon motions associated with the ground and excited electronic states, as in the time-domain version of the Fermi golden rule [35]. Both the squared coupling and the correlation function depend on the phonon kinetic energy, but in the opposite ways. In the semiclassical description [23,35], the squared coupling increases with temperature, but the correlation function also decays faster, resulting in the cancellation.

The moderate temperature dependence of the nonradiative decay rate seen in our calculations agrees well with the excited state lifetime experiments, e.g., Fig. 5(b) of Ref. [8], Fig. 2 of Ref. [5], Fig. 4 of [6] and Table 1 of Ref. [9]. Our result also agrees with the PL intensity data reported in Ref. [7], although other authors [4] observe much stronger dependence of PL intensity on temperature. According to our calculations, the weak temperature dependence of the PL intensity is due to the weak temperature dependence of nonradiative decay, rather than insignificant nonradiative decay channels, as thought originally [7]. Note that in contrast to the PL decay, the PL linewidth is determined by the pure-dephasing time rather than by the excited state lifetime [34] and dramatically decreases at low temperatures [44].

Our simulation results fall within the range of the experimental data [3–6,11,12,14,15], still, a number of approximations may have influenced the estimated decay times. The relaxation rate shows very strong dependence on the pure-dephasing time, Table I. Although the estimated times are in good agreement with the experimental linewidths [34], the semiclassical scheme used to incorporate the dephasing effect into the TDDFT simulation was very simple. This is the first implementation of decoherence into TDDFT, and more sophisticated approaches carry significant computational expense. It was also assumed that the decay bottleneck is determined by the transition from the lowest singlet excited state to the ground state. Other states can be thermally accessible from the lowest excited state [10], and the decay can occur from several states simultaneously. Additionally, singlet states may decay into the lower-energy triplet manifold [45] via intersystem crossing induced by spin-orbit coupling. Triplets are typically longer lived than singlets and

TABLE I. Pure-dephasing and nonradiative relaxation times of the first excitation in the (6,4) CNT with and without defects at low and ambient temperatures. The first two rows show the dephasing times [34] and the relaxation times calculated using these dephasing times. The third and fourth rows provide a comparison of the relaxation time scales calculated with the dephasing time fixed at 0.01 and 0.5 ps, respectively.

	Ideal	7557	SW	Ideal, 50 K
Dephasing time (ps)	0.060	0.018	0.048	0.995
Relaxation time (ps)	147	41.5	66.7	170
Relaxation (ps) with 0.01 ps dephasing	716	77.5	251	4906
Relaxation (ps) with 0.50 ps dephasing	39.8	3.55	16.2	258

may account for the nanosecond components in the experimental data.

In summary, we pioneered a time-domain *ab initio* atomistic simulation of fluorescence quenching in a semiconducting CNT by nonradiative decay, directly mimicking the time-resolved experiments. In order to study the long-time decay process, we included quantum decoherence effects into TDDFT, also for the first time. Our simulations showed that strong nonradiative channels exist in CNTs. PL quenching is substantially enhanced by defects, which are likely to be responsible for multiple decay time scales and low PL yields seen in the experiments. The nonradiative decay shows weak temperature dependence, since it is promoted by high-frequency vibrational modes. Vibrationally induced dephasing in the electronic subsystem strongly influences the PL quenching rate, suggesting that both defects and local environment can be very important in the PL experiments on CNTs.

The research was supported by grants from NSF No. CHE-0701517, IGERT and ACS-PRF No. 46772-AC6. O. V. P. is grateful to Professor Yoshitaka Tanimura for hosting the JSPS visit at the Kyoto University during manuscript preparation.

*Corresponding author.
prezhdo@u.washington.edu

[1] M. J. O'Connell *et al.*, Science **297**, 593 (2002).
[2] J. Lefebvre, Y. Homma, and P. Finnie, Phys. Rev. Lett. **90**, 217401 (2003).
[3] A. Hagen *et al.*, Phys. Rev. Lett. **95**, 197401 (2005).
[4] S. Berger *et al.*, Nano Lett. **7**, 398 (2007).
[5] Y.-Z. Ma *et al.*, Phys. Chem. Chem. Phys. **8**, 5689 (2006).
[6] H. Hirori *et al.*, Phys. Rev. Lett. **97**, 257401 (2006).
[7] J. Lefebvre, P. Finnie, and Y. Homma, Phys. Rev. B **70**, 045419 (2004).
[8] W. K. Metzger *et al.*, J. Phys. Chem. C **111**, 3601 (2007).
[9] D. Karaiskaj *et al.*, Phys. Rev. B **75**, 113409 (2007).
[10] I. B. Mortimer and R. J. Nicholas, Phys. Rev. Lett. **98**, 027404 (2007).
[11] F. Wang *et al.*, Phys. Rev. Lett. **92**, 177401 (2004).
[12] M. Jones *et al.*, Phys. Rev. B **71**, 115426 (2005).
[13] J. Lefebvre *et al.*, Nano Lett. **6**, 1603 (2006).
[14] H. Y. Seferyan *et al.*, Nano Lett. **6**, 1757 (2006).
[15] M. Jones *et al.*, Nano Lett. **7**, 300 (2007).
[16] C. D. Spataru *et al.*, Phys. Rev. Lett. **95**, 247402 (2005).
[17] V. Perebeinos, J. Tersoff, and P. Avouris, Nano Lett. **5**, 2495 (2005).
[18] C. F. Craig, W. R. Duncan, and O. V. Prezhdo, Phys. Rev. Lett. **95**, 163001 (2005).
[19] E. Tapavicza, I. Tavernelli, and U. Rothlisberger, Phys. Rev. Lett. **98**, 023001 (2007).
[20] E. Runge and E. K. U. Gross, Phys. Rev. Lett. **52**, 997 (1984).
[21] J. C. Tully, J. Chem. Phys. **93**, 1061 (1990).
[22] P. V. Parahdekar and J. C. Tully, J. Chem. Phys. **122**, 094102 (2005).
[23] O. V. Prezhdo and P. J. Rossky, Phys. Rev. Lett. **81**, 5294 (1998).
[24] O. V. Prezhdo, Phys. Rev. Lett. **85**, 4413 (2000).
[25] G. Katz, M. A. Ratner, and R. Kosloff, Phys. Rev. Lett. **98**, 203006 (2007).
[26] M. Sternberg *et al.*, Phys. Rev. Lett. **96**, 075506 (2006).
[27] B. F. Habenicht, C. F. Craig, and O. V. Prezhdo, Phys. Rev. Lett. **96**, 187401 (2006).
[28] G. Kresse and J. Furthmüller, Comput. Mater. Sci. **6**, 15 (1996).
[29] Y. Miyamoto, A. Rubio, and D. Tomanek, Phys. Rev. Lett. **97**, 126104 (2006).
[30] A. V. Krasheninnikov, Y. Miyamoto, and D. Tomanek, Phys. Rev. Lett. **99**, 016104 (2007).
[31] O. Pulci *et al.*, Phys. Rev. Lett. **81**, 5374 (1998).
[32] C. D. Spataru *et al.*, Phys. Rev. Lett. **92**, 077402 (2004).
[33] E. B. Barros *et al.*, Phys. Rev. B **73**, 241406 (2006).
[34] B. F. Habenicht *et al.*, Nano Lett. **7**, 3260 (2007).
[35] O. V. Prezhdo and P. J. Rossky, J. Chem. Phys. **107**, 5863 (1997).
[36] R. E. Larsen and B. J. Schwartz, J. Phys. Chem. B **110**, 9692 (2006).
[37] S. Y. Kim and S. Hammes-Schiffer, J. Chem. Phys. **124**, 244102 (2006).
[38] H. Kamisaka *et al.*, Nano Lett. **6**, 2295 (2006).
[39] S. Mukamel, *Principles of Nonlinear Optical Spectroscopy* (Oxford University Press, New York, 1995).
[40] M. Vandescuren *et al.*, Carbon **45**, 349 (2007).
[41] E. W. Streed *et al.*, Phys. Rev. Lett. **97**, 260402 (2006).
[42] S. Maniscalco, J. Piilo, and K. A. Suominen, Phys. Rev. Lett. **97**, 130402 (2006).
[43] L. Cognet *et al.*, Science **316**, 1465 (2007).
[44] H. Htoon *et al.*, Phys. Rev. Lett. **93**, 027401 (2004).
[45] S. Tretiak, Nano Lett. **7**, 2201 (2007).